Supporting Information for

Sulfolipid-1 Biosynthesis Restricts *Mycobacterium tuberculosis* Growth in Human Macrophages

Sarah A. Gilmore[*], *Michael W. Schelle*[†], *Cynthia M. Holsclaw*[¶], *Clifton D. Leigh*[†], *Madhulika Jain*[□], *Jeffery S. Cox* [□], *Julie A. Leary*[¶,§], *and Carolyn R. Bertozzi*[*, †, ‡,1]

Departments of Chemistry[†] and Molecular and Cell Biology[*], Howard Hughes Medical Institute[‡], University of California, Berkeley, CA 94720; Section of Molecular and Cell Biology[¶] and Department of Chemistry[§], University of California, Davis, CA 95616; and Department of Microbiology and Immunology[□], University of California, San Francisco, CA 94143.

[1]To whom correspondence may be addressed: University of California, B84 Hildebrand Hall, #1460, Berkeley, CA 94720. Tel: (510) 643-1682. Fax: (510) 643-2628. E-mail: crb@berkeley.edu

Supplemental Figure Legends

Figure S1. Model of SL-1 biosynthesis
Free trehalose is sulfated by Stf0 to form T2S. PapA2 then acylates the 2'-position of T2S to form SL_{659}. Pks2 synthesizes a (hydroxy)phthioceranic acid which is transferred directly by PapA1 onto SL_{659} to form SL_{1278}. The diacylated SL_{1278} is then transferred by the putative lipid transporter MmpL8 to the exterior of the cell wall where the two final acylation reactions occur to yield fully elaborated SL-1.

Figure S2. MALDI-TOF MS of purified SL-1
SL-1 was enriched by anion-exchange chromatography and further purified via HPLC silica column. SL-1 is observed as a collection of lipoforms that vary in the lengths of their acyl groups (± 14 mass units).

Figure S3. SL-1 does not modulate pro-inflammatory cytokine production *in vitro*

hiDCs, human primary macrophages, the human monocyte THP-1 cell line, or the murine macrophage RAW264.7 cell line were cultured with SL-1, SL-A, or LPS. Levels of TNF produced by each cell type in response to the indicated stimulus were evaluated by ELISA. Data are representative of at least two independent experiments performed in triplicate, with human cells derived from different donors where appropriate. Error bars represent the standard deviation from the mean.

Figure S4. Qualitative MS analysis of *stf0* mutant for T2S and PDIM
(a) Disruption of *stf0* abolishes trehalose-2-sulfate (T2S) production. FT-ICR MS of chloroform: methanol extracts of WT, Δ*stf0*, and Δ*stf0* + p*stf0* strains verify loss of T2S (m/z=421.06), as denoted by an asterisk, from Δ*stf0*. The other species observed in Δ*stf0* and the Δ*stf0* + p*stf0* strains is a phosphorylated disaccharide that is not visible in WT samples due to ion suppression that occurs when analyzing complex lipid extracts. (b) PDIM synthesis is intact in the Δ*stf0* mutant. FT-ICR analysis of surface-extractable lipids reveals that PDIM retains the same average m/z= 1402 in the Δ*stf0* mutant as compared to WT.

Figure S5. Δ*stf0* displays no *in vitro* growth defects
The *in vitro* growth rates of Δ*stf0*, WT, and Δ*stf0* + p*stf0* Mtb were approximated by measuring their optical density at 600 nm over time. Data are representative of three independent experiments.

Figure S6. **Δ***papA2* is more resistant to LL-37 compared to WT Mtb.
The indicated strains of Mtb were exposed to increasing concentrations (0, 6.5, and 65 μg/mL) of LL-37. After 3 days, Mtb viability was measured by plating bacteria on solid agar to enumerate cfu counts. Data are representative three biological replicates. Error bars correspond to the means (± s.d.). *, P=0.329 (not significant) for the comparison of Δ*papA2* versus WT; **, P=0.018 for the comparison of Δ*papA2* versus WT.

Figure S7. Stf0 displays no trafficking defects compared to WT *in vivo*
Liver (a) and spleen (b) cfu counts for BALB/c mice infected via aerosol with WT or Δ*stf0* Mtb. Each data point represents the average cfu count from 4-5 mice, and error bars indicate the standard deviation from the mean.

Table Legend

Table S1. Top 50 most highly upregulated microarray gene identities.
Identities of the 50 most highly up regulated, statistically significant ($p<0.02$) genes induced in hiDCs by SL-1, SL-A, or P3K as represented in Figure 2.

Supplemental Figures

Figure S1

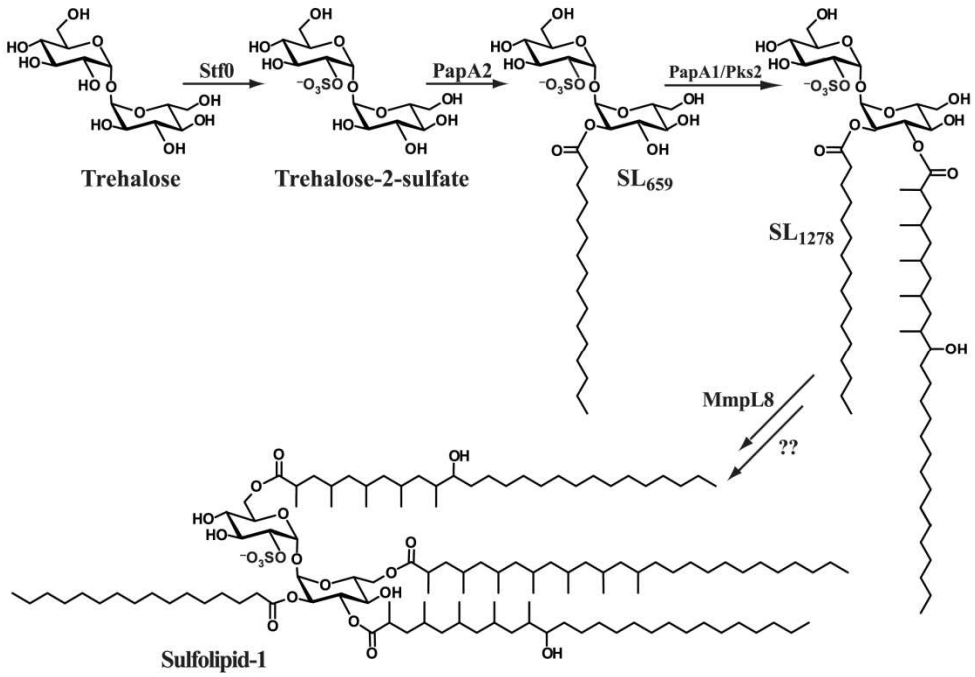

Figure S2

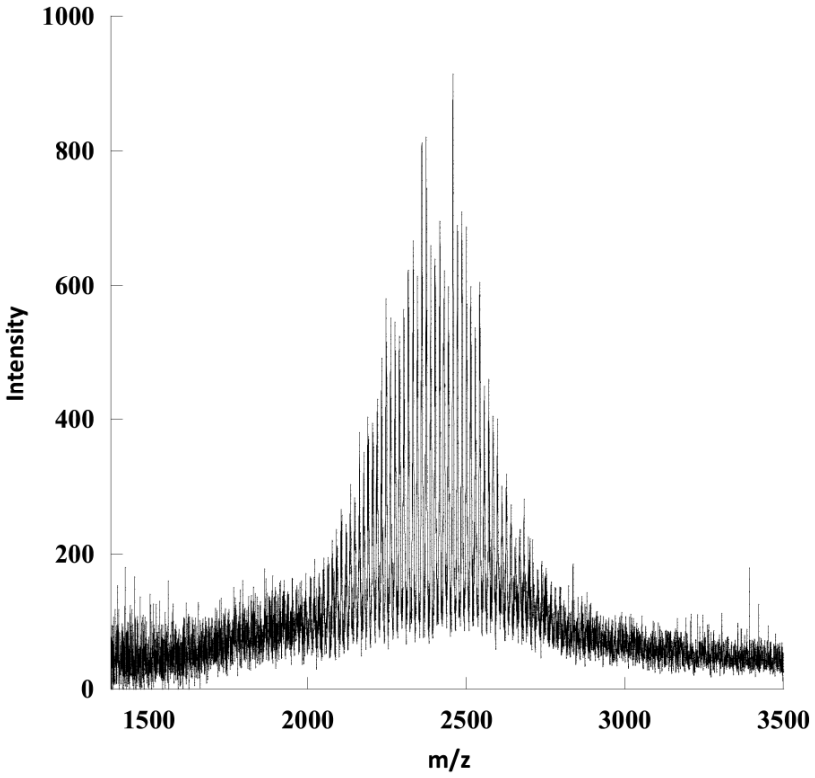

Figure S3

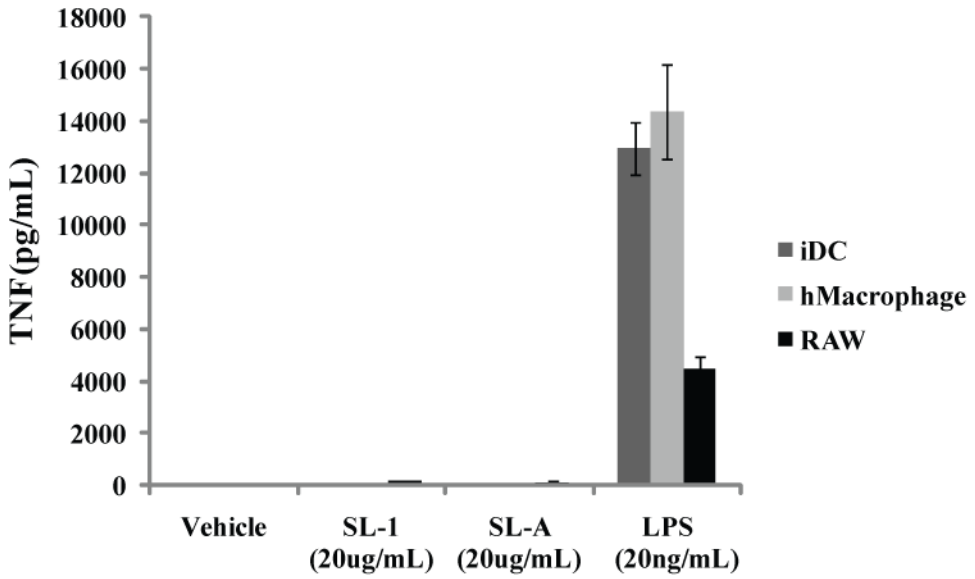
18000
16000
14000
12000
10000
8000
6000
4000
2000
0
TNF (pg/mL)
Vehicle
SL-1 (20ug/mL)
SL-A (20ug/mL)
LPS (20ng/mL)
iDC
hMacrophage
RAW

Figure S4.

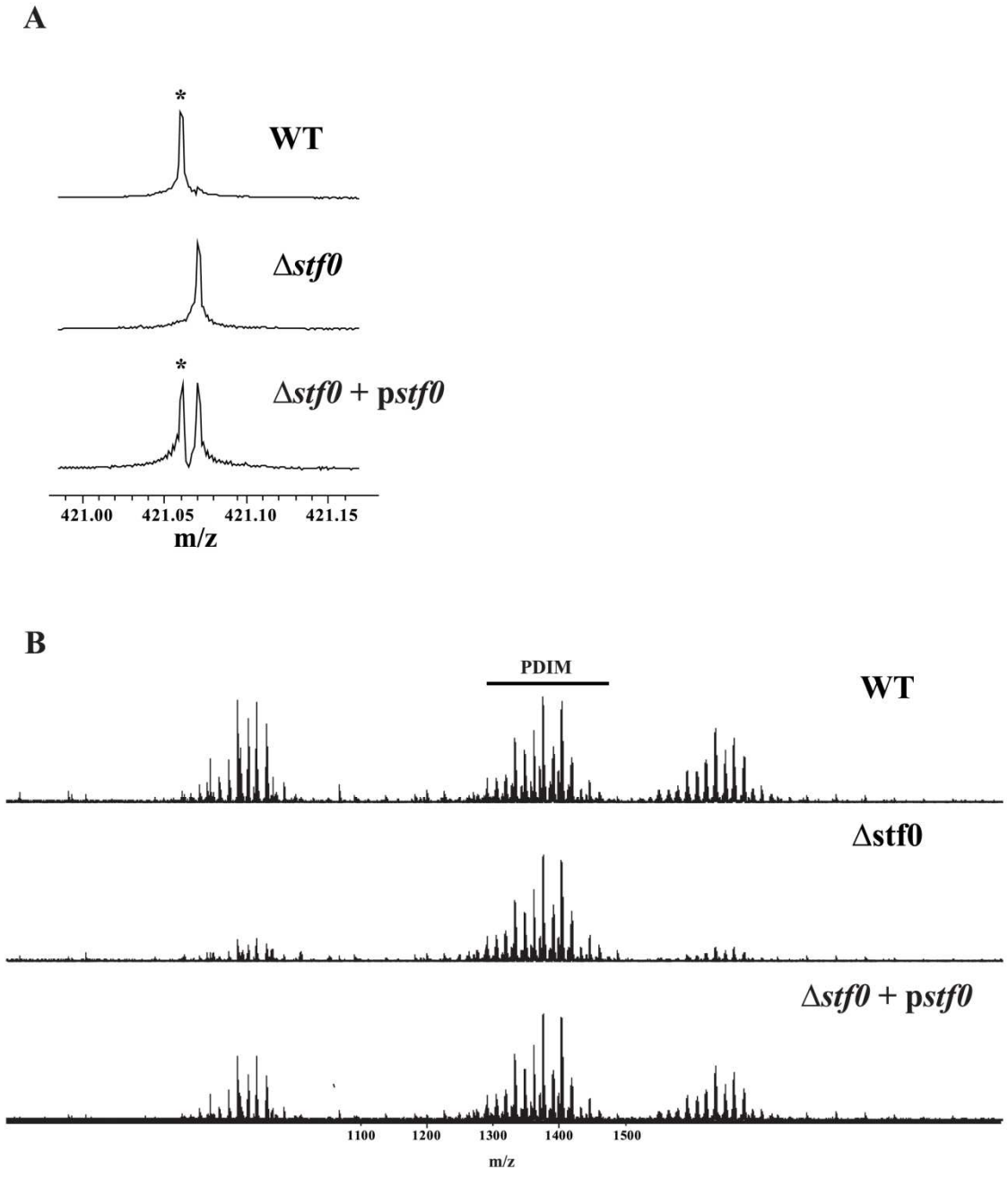
A
*
WT
Δstf0
*
Δstf0 + pstf0
421.00
421.05
421.10
421.15
m/z
B
PDIM
WT
Δstf0
Δstf0 + pstf0
1100
1200
1300
1400
1500
m/z

Figure S5.

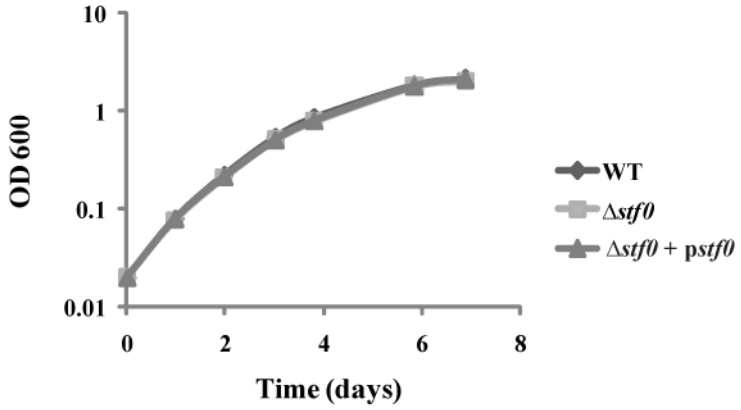

Figure S6

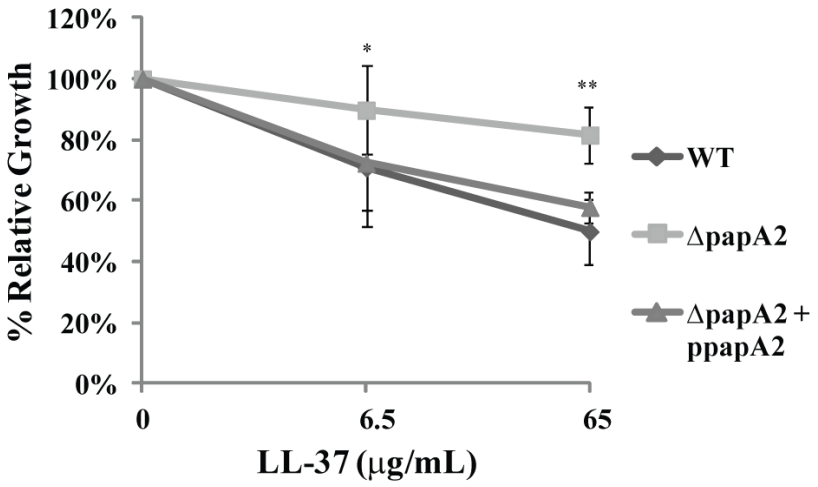
120%
100%
80%
60%
40%
20%
0%
% Relative Growth
*
**
0
6.5
65
LL-37 (μg/mL)
WT
ΔpapA2
ΔpapA2 + ppapA2

Figure S7

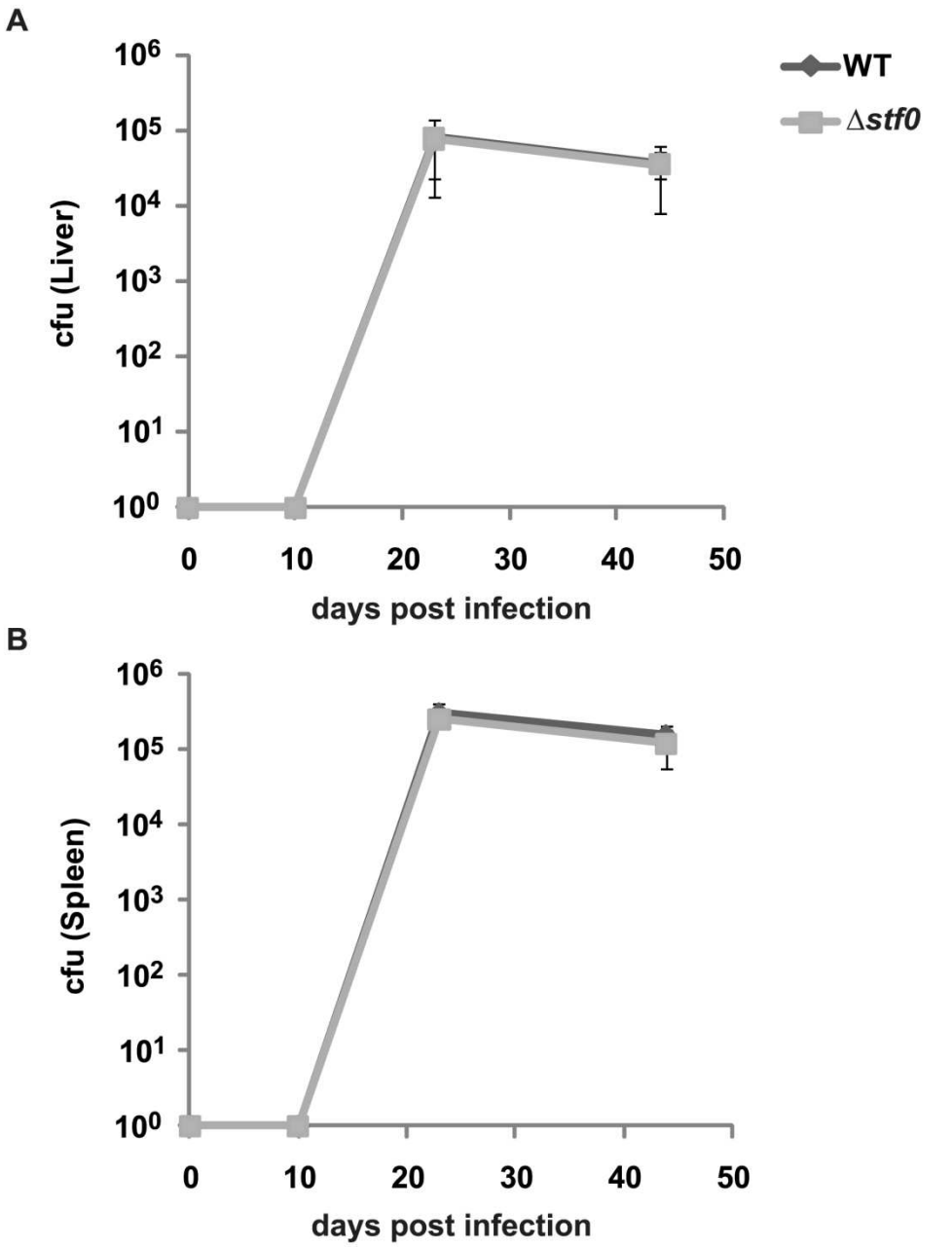

Supplemental Table

Table S1.

Top 50 genes upregulated in response to P3K	Gene Name	Gene
Proinflammatory/vasoactive		
	interleukin 6 (interferon, beta 2)	IL6
	interleukin 1, beta	IL1B
	tumor necrosis factor, alpha-induced protein 6	TNFAIP6
	interleukin 8	IL8
	colony stimulating factor 2 (granulocyte-macrophage)	CSF2
	interleukin 1, alpha	IL1A
	tenascin C (hexabrachion)	TNC
	plasminogen activator, tissue	PLAT
	serpin peptidase inhibitor, clade B (ovalbumin), member 2	SERPINB2
	matrix metallopeptidase 7 (matrilysin, uterine)	MMP7
	prostaglandin-endoperoxide synthase 2 (COX-1)	PTGS2
	interleukin 1 family, member 9	IL1F9
	tumor necrosis factor (TNF superfamily, member 2)	TNF
	GTP cyclohydrolase 1 (dopa-responsive dystonia)	GCH1
	tumor necrosis factor, alpha-induced protein 2	TNFAIP2
	interleukin 18 receptor 1	IL18R1
	interleukin 23, alpha subunit p19	IL23A
	sphingosine-1-phosphate phosphotase 2	SGPP2
	glycoprotein Ib (platelet), alpha polypeptide (CD42b)	GP1BA
Chemotaxis/Cell Migration		
	chemokine (C-C motif) ligand 20	CCL20
	chemokine (C-C motif) ligand 1	CCL1
	chemokine (C-X-C motif) ligand 1	CXCL1
	chemokine (C-X-C motif) ligand 3	CXCL3
	chemokine (C-X-C motif) ligand 2	CXCL2
	intercellular adhesion molecule 1 (CD54)	ICAM1
	ADAM metallopeptidase domain 19 (meltrin beta)	ADAM19
Antigen Presentation/ /T-cell co-stimulation		
	tumor necrosis factor receptor superfamily,	TNFRSF4

	member 4 (OX40)	
	pentraxin-related gene, rapidly induced by IL-1 beta	PTX3
	thymic stromal lymphopoietin	TSLP
	interleukin 7 receptor	IL7R
Anti-inflammatory		
	adenosine A2a receptor	ADORA2A
	B-cell CLL/lymphoma 3	BCL3
	superoxide dismutase 2, mitochondrial	SOD2
	TNFAIP3 interacting protein 3	TNIP3
	nuclear factor of kappa light polypeptide gene enhancer in B-cells 1 (p105)	NFKB1
	nuclear factor of kappa light polypeptide gene enhancer in B-cells inhibitor, zeta	NFKBIZ
Signaling/Metabolism		
	IBR domain containing 2	IBRDC2
	EH-domain containing 1	EHD1
	sphingosine-1-phosphate phosphotase 2	SGPP2
	ankyrin repeat and BTB (POZ) domain containing 2	ABTB2
	ELOVL family member 7, elongation of long chain fatty acids (yeast)	ELOVL7
	shroom	SHRM
	arrestin domain containing 3	ARRDC3
	wingless-type MMTV integration site family, member 5A	WNT5A
	baculoviral IAP repeat-containing 3 (cIAP2)	BIRC3
	guanylate binding protein 3	GBP3
	G0/G1switch 2	G0S2
	RAS guanyl releasing protein 1 (calcium and DAG-regulated)	RASGRP1
	ankyrin repeat domain 15	ANKRD15
	Wilms tumor 1 associated protein	WTAP
Top 50 genes upregulated in response to SL-1	**Gene Name**	**Gene**
Chemotaxis/Cell Migration		
	fucosyltransferase 7 (alpha (1,3) fucosyltransferase)	FUT7
	integrin, beta 1 (antigen CD29)	ITGB1
	interleukin 8 receptor, beta	IL8RB
	cadherin 12, type 2 (N-cadherin 2)	CDH12
	hyaluronan and proteoglycan link protein 3	HAPLN3

Metabolism		
	heat shock protein 90kDa alpha (cytosolic), class A member 1	HSP90AA1
	pyruvate dehydrogenase kinase, isozyme 4	PDK4
	cell division cycle associated 7-like	CDCA7L
	aldehyde dehydrogenase (succinate-semialdehyde dehydrogenase)	ALDH5A1
	heme oxygenase (decycling) 1	HMOX1
	paired box gene 8	PAX8
	pericentriolar material 1	PCM1
	transmembrane protein 97	TMEM97
	solute carrier family 26, member 10	SLC26A10
	24-dehydrocholesterol reductase	DHCR24
Antigen Presentation		
	CD1d molecule	CD1D
	CD84 molecule	CD84
	anti-rabies SO57 immunoglobulin heavy chain	IGHG1
Unknown function		
	hypothetical gene supported by AK124070	LOC400707
	hypothetical protein FLJ38663	FLJ38663
	chromosome 8 open reading frame 70	C8orf70
	hypothetical protein MGC33584	MGC33584
	neuroblastoma breakpoint family, member 11	NBPF11
	translocation associated membrane protein 1-like 1	TRAM1L1
	fibronectin type III domain containing 5	FNDC5
	neuroblastoma breakpoint family, member 3	NBPF3
	tetratricopeptide repeat domain 23	TTC23
	immediate early response 5-like	IER5L
	CTAGE family, member 5	CTAGE5
	XAGE-4 protein	RP11-167P23.2
	bromodomain containing 3	BRD3
	trinucleotide repeat containing 15	TNRC15
Cell Cytoskeleton/Endocytosis		
	tropomyosin 1 (alpha)	TPM1
	villin 2 (ezrin)	VIL2
	sorting nexin 24	SNX24
	membrane protein, palmitoylated 5	MPP5
	intersectin 1 (SH3 domain protein)	ITSN1

Signaling		
	protein tyrosine phosphatase, receptor type, N	PTPRN
	RAB32, member RAS oncogene family	RAB32
	Ras and Rab interactor 1	RIN1
	sphingolipid G-protein-coupled receptor, 8	EDG8
	GTPase activating protein and VPS9 domains 1	GAPVD1
	protein phosphatase 1, regulatory (inhibitor) subunit 11	PPP1R11
	G protein-coupled receptor 120	GPR120
	ralA binding protein 1	RALBP1
	protein phosphatase 1, regulatory (inhibitor) subunit 14A	PPP1R14A
	SRY (sex determining region Y)-box 17	SOX17
	coiled-coil domain containing 50	CCDC50
	wingless-type MMTV integration site family, member 5B	WNT5B
	fused toes homolog (mouse)	FTS
Top 50 genes upregulated in response to SL-A	**Gene Name**	**Gene**
Metabolism/Cell Cycle		
	serine/arginine repetitive matrix 1	SRRM1
	cytochrome P450, family 2, subfamily C, polypeptide 19	CYP2C19
	eukaryotic translation initiation factor 2A, 65kDa	EIF2A
	pericentriolar material 1	PCM1
	heat shock protein 90kDa alpha (cytosolic), class B member 1	HSP90AB1
	heat shock protein 90kDa alpha (cytosolic), class A member 1	HSP90AA1
	oxidation resistance 1	OXR1
	hydroxyacyl-Coenzyme A dehydrogenase	HADHA
	poly (ADP-ribose) polymerase family, member 14	PARP14
	prothymosin, alpha (gene sequence 28)	PTMA
	N-acetylglucosamine-1-phosphate transferase, alpha and beta subunits	GNPTAB
	similar to cell division cycle 10 homolog	LOC441220
	Nipped-B homolog (Drosophila)	NIPBL
	potassium voltage-gated channel, subfamily G, member 1	KCNG1
Antigen Presentation/Pathogen		

Recognition		
	Fc receptor-like 1	FCRL1
	anti-rabies SO57 immunoglobulin heavy chain	IGHG1
Unknown function		
	chromosome X open reading frame 22	CXorf22
	testicular cell adhesion molecule 1 homolog (mouse)	TCAM1
	heat shock protein 90kDa alpha (cytosolic), class B member 3 (pseudogene)	HSP90AB3P
	neuroblastoma breakpoint family, member 3	NBPF3
	hypothetical protein LOC338809	LOC338809
	zinc finger protein 560	ZNF560
	RNA binding motif protein 24	RBM24
	trinucleotide repeat containing 15	TNRC15
	P antigen family, member 2 (prostate associated)	PAGE2
	KIAA0319-like	KIAA0319L
	hypothetical protein FLJ38663	FLJ38663
	hypothetical protein LOC283874	LOC283874
	chromosome 8 open reading frame 70	C8orf70
	chromosome 20 open reading frame 23	C20orf23
Cell Cytoskeleton/Endocytosis		
	villin 2 (ezrin)	VIL2
	intersectin 1 (SH3 domain protein)	ITSN1
	tropomyosin 1 (alpha)	TPM1
	syntaxin 2	STX2
	RANBP2-like and GRIP domain containing 5	RGPD5
	transforming, acidic coiled-coil containing protein 1	TACC1
	sorting nexing 24	SNX24
	WAS protein homology region 2 domain containing 1	WHDC1
Signaling/Transcription		
	coiled-coil domain containing 50	CCDC50
	RAB11 family interacting protein 2 (class I)	RAB11FIP2
	high mobility group AT-hook 1	HMGA1
	PHD finger protein 2	PHF2
	RAB11 family interacting protein 1 (class I)	RAB11FIP1
	dishevelled associated activator of morphogenesis 2	DAAM2
	cholinergic receptor, nicotinic, alpha 1 (muscle)	CHRNA1

	protein tyrosine phosphatase, receptor type, E	PTPRE
	acidic (leucine-rich) nuclear phosphoprotein 32 family, member B	ANP32B
	similar to Acidic leucine-rich nuclear phosphoprotein 32 family member B	LOC646791
	A kinase (PRKA) anchor protein 13	AKAP13
Anti-inflammatory		
	FK506 binding protein 5	FKBP5

Supplemental Materials and Methods

Determination of Mtb growth rates *in vitro*. Mtb was grown to late log phase, washed twice in PBS and pelleted by centrifugation at low speed to remove clumps. The OD_{600} was adjusted to 0.02 in 50 mL of complete 7H9 media and the growth of each strain was approximated by measuring the OD_{600} every 24-48 hours.

Generation of human primary macrophages and immature dendritic cells. Total human peripheral blood mononuclear cells (PBMCs) were obtained as buffy coats from the American Red Cross, Oakland, CA. PBMCs were prepared by sedimentation of erythrocytes with Dextran T500 and separation over a Ficoll-Hypaque gradient. Total monocytes were obtained by negative isolation using Dynal Monocyte MyPure Negative Isolation Kit (Invitrogen) and cultured in AIM-V media supplemented with 1% human AB serum and 20-50 ng mL^{-1} of M-CSF to generate macrophages or 500U mL^{-1} IL-4 and 1000U mL^{-1} GM-CSF to generate hiDCs. Media was replaced on days 2 and 4 of culture to replenish growth factors.

SL-1 purification. Approximately 5 g of □-irradiated Mtb H37Rv whole cells (Colorado State University) were extracted in 100mL chloroform: methanol (1:1, v/v) at room temperature for 2 h. The organic layer was filtered 3 times by vacuum filtration, concentrated, and further partitioned between chloroform and water to constitute the total Mtb lipid extract. 40 mg of lipid extract was resuspended in chloroform/methanol (4:1, v/v) and passed over an anion-exchange column (AG4-X4 resin, 100–200 mesh, biotechnology grade, free-base form, Bio-RAD) that was pre-charged with chloroform/methanol/acetic acid (400:100:0.6, v/v). The column was washed with chloroform/methanol (4:1, v/v) and binders were eluted using a gradient of 2–5 mM triethylamine in chloroform/methanol (4:1, v/v). Fractions were mixed (1:1, v/v) with matrix solution (10 mg ml^{-1} 2-[4-Hydroxyphenylazo] benzoic acid) and analyzed by matrix assisted laser desorption ionization time-of-flight mass spectrometry (MALDI-TOF MS, Applied Biosystems Voyager DE Pro). Fractions containing SL-1 were pooled and further purified by HPLC on a silica column (Varian Microsorb 100, particle size 5µm). Prior to injection, the column was first equilibrated in chloroform/methanol (98:2, v/v) and SL-1 was eluted with a 2-27% methanol gradient over 30 minutes. Fractions were collected and analyzed for purity by MALDI as well as by TLC using a 60:12:1 (v/v) chloroform: methanol: water solvent system.

Stimulation of leukocytes with SL-1, SL-A, or LPS. 4 x 10^5 hiDCs, human primary macrophages, THP-1, or RAW264.7 cells were treated with 20µg mL^{-1} SL-1, 20µg mL^{-1} SL-A that had been dissolved in petroleum ether and allowed to evaporate off the bottom of a cell culture dish or 20ng mL^{-1} LPS as indicated. After 24 hours, the amount of TNF elicited by each cell type was analyzed by ELISA according to the manufacturer's recommendations (BD Bioscience).

Δ*papA2* Antimicrobial Peptide Susceptibility

The construction of Δ*papA2* in the Erdman strain of Mtb was reported in (1). For complementation of Δ*papA2*, the *papA2* gene was cloned from Mtb into the integrating mycobacterial expression vector pMV306 under the control of its putative endogenous promoter (2). This plasmid was electroporated into Δ*papA2*, and transformants were selected on kanamycin-containing plates. Sensitivity of Mtb to antimicrobial peptides was assayed as previously described (3). Briefly, Mtb was grown to late-log phase, washed in PBS, and pelleted by centrifugation at low speed to remove clumps. Cells ($2x10^6$) of each strain were exposed to the indicated concentration of LL-37 (AnaSpec) dissolved in RPMI: water (1:4, v/v) at 37 °C. After three days, bacteria were plated on solid agar to enumerate the number of viable bacteria by cfu counts.

Microarray Preparation, Array Hybridizations, and Analysis

Microarray sample preparation, labeling, and array hybridizations were performed according to standard protocols from the UCSF Shared Microarray Core Facilities and Agilent Technologies (http://www.arrays.ucsf.edu and http://www.agilent.com). RNA was amplified and labeled with Cy3-CTP using the Agilent low RNA input fluorescent linear amplification kits following the manufacturer's protocol. Labeled cRNA was assessed using the Nandrop ND-100 (Nanodrop Technologies, Inc.), and equal amounts of Cy3 labeled target were hybridized to Agilent whole human genome 4x44K arrays. Arrays were scanned using the Agilent microarray scanner and raw signal intensities were extracted with Feature Extraction v9.1 software. The dataset was normalized using the *quantile* normalization method that is proposed by Bolstad et al. (4). No background subtraction was performed, and the median feature pixel intensity was used as the raw signal before normalization. A small number of probes (245) have replicate spots, and these were summarized by taking the median intensity. A linear model was fit to the comparison to estimate the mean M values and calculated moderated t-statistic, B statistic, false discovery rate and p-value for each gene for the comparison of interest. All procedures were carried out using functions in the R package *limma in Bioconductor* (5,6).

Supplemental References

1.Kumar, P., Schelle, M. W., Jain, M., Lin, F. L., Petzold, C. J., Leavell, M. D., Leary, J. A., Cox, J. S., and Bertozzi, C. R. (2007) PapA1 and PapA2 are acyltransferases essential for the biosynthesis of the Mycobacterium tuberculosis virulence factor sulfolipid-1, *Proc Natl Acad Sci U S A 104*, 11221-11226.

2.Stover, C. K., de la Cruz, V. F., Fuerst, T. R., Burlein, J. E., Benson, L. A., Bennett, L. T., Bansal, G. P., Young, J. F., Lee, M. H., Hatfull, G. F., and et al. (1991) New use of BCG for recombinant vaccines, *Nature 351*, 456-460.

3. Liu, P. T., Stenger, S., Li, H., Wenzel, L., Tan, B. H., Krutzik, S. R., Ochoa, M. T., Schauber, J., Wu, K., Meinken, C., Kamen, D. L., Wagner, M., Bals, R., Steinmeyer, A., Zugel, U., Gallo, R. L., Eisenberg, D., Hewison, M., Hollis, B. W., Adams, J. S., Bloom, B. R., and Modlin, R. L. (2006) Toll-like receptor triggering of a vitamin D-mediated human antimicrobial response, *Science 311*, 1770-1773

4. Bolstad BM, Irizarry RA, Astrand M, Speed TP (2003) A comparison of normalization methods for high density oligonucleotide array data based on variance and bias. *Bioinformatics* 19:185-193.

5. Gentleman, R. C., Carey, V. J., Bates, D. M., Bolstad, B., Dettling, M., Dudoit, S., Ellis, B., Gautier, L., Ge, Y., Gentry, J., Hornik, K., Hothorn, T., Huber, W., Iacus, S., Irizarry, R., Leisch, F., Li, C., Maechler, M., Rossini, A. J., Sawitzki, G., Smith, C., Smyth, G., Tierney, L., Yang, J. Y., and Zhang, J. (2004) Bioconductor: open software development for computational biology and bioinformatics, *Genome biology 5*, R80.

6. Smyth, G. K. (2004) Linear models and empirical bayes methods for assessing differential expression in microarray experiments, *Statistical applications in genetics and molecular biology 3*, Article3.